

Structural, Photoluminescence and Optical Properties of CdSe:Zn Nanoparticles: Effects of Doping Concentrations

Nimrod Gitonga¹, Sharon Kiprotich^{1,*}, Michael Musembi²

¹Department of Physical and Biological science, Murang'a University of Technology, Murang'a, Kenya

²Department of Physics Machakos University, Machakos, Kenya

Abstract The concentration of dopant introduced into the host nanoparticle alters its structural, optical and morphological properties. This paper explains the one pot synthesis of zinc doped cadmium selenide nanoparticles (Zn-CdSeNPs) using L-cysteine as capping agent. The synthesis process was carried out with three necked flask at 90°C. The X-ray diffraction (XRD) pattern confirms the formation of zinc blende cubic structure. Scherrer equation was used to calculate crystal size, and the results showed that crystal size decreased with an increase in dopant concentration. Pure CdSe nanoparticles had a crystal size of 24.66 nm and 15% Zinc doped CdSe had a crystal size of 17.72nm. Results from photoluminescence (PL) spectroscopy shows that at high concentration of Zn dopant, the emission peak shift to higher wavelength and the intensity of the peak decreased. 1% zinc doped CdSe nanoparticles had the highest intensity while 15% Zn-CdSe nanoparticles had the lowest PL intensity. The optical properties of Zn-CdSeNPs were characterized with Ultra Violet visible spectroscopy. Tauc's plot was used to obtain the bandgap energies of nanoparticles. The results showed that at 11% Zn-CdSe the bandgap energy was 1.35 eV and at lower dopant concentration 1% the bandgap energy was 1.92 eV.

Keywords Bandgap, Dopants, Optical properties, Cadmium selenide, Zinc blende, Nanoparticles

1. Introduction

Since the rise in nanotechnology, scholars and researchers around the world have sought to invent new nanomaterials and improve the properties of the existing nanomaterials. Nanotechnology has made human life easier by changing the size and properties of so many devices used either in health, electronics or agricultural activities [1]. The need for this improvement and new invention is a fascinating task for research community. Group II-VI semiconducting elements have good photovoltaic and optoelectronic properties [2]. The nanomaterials of these semiconductors are being pursued due to their ability to control their morphology and shape. CdSe material has bandgap energy comparable with solar energy spectrum [3], adjustable n and p type of conductivity depending on the dopant [4] and high absorption coefficient in visible and infrared region [5]. In the last decade CdSe nanoparticles has attracted attentions of researchers due to its wide applications in solar cells [6], gas sensors [7] and photodetector [8]. As of 2020 the power conversion efficiency (PCE) of perovskite solar cells was 25%. This is considered low since the amount of energy produce by sun in one hour is more than the energy consumed by the world in a year [9].

Therefore other measures should be taken into consideration to ensure efficiency of this power conversion is increased to reduce the use of fossil fuels which has led to climate change.

CdSe nanoparticles degrade when exposed to sunlight for a very long time thus decreasing the efficiency of solar cells. They also have lower conversion efficiency when compared to other nanoparticles such silicon [10]. To improve CdSe nanoparticles properties for solar cells application, several factors such as method of preparation, use of dopant, growth temperature and annealing temperature are being considered. CdSe nanoparticles have been successfully prepared via different methods such as thermal treatment technique [11], wet chemical colloidal method [12], sol gel method [13] and green synthesis method [14]. The best method to obtain better quality and highly structured materials of CdSe nanoparticles is still ongoing.

Introducing alien element to semiconductors has tremendous effects on the optical, morphological and electronic properties. For example when Zhao et al., (2019) [15] prepared Ag doped CdSe quantum dots, it was observed that incorporation of Ag into core region leads to metallic-like electronic properties. Several transitional metals are used as dopants in CdSe nanoparticles to modify the optical, electronic and magnetic properties of CdSe. They include Ag, Mn, Co, and Ni. In this study zinc was used as dopant in CdSe nanoparticles used in solar cell application because Zn^{2+} has smaller ionic radius (0.74\AA) compared to Cd^{2+} (0.95\AA) thus the lattice contraction

* Corresponding author:

Skiprotich@mut.ac.ke (Sharon Kiprotich)

Received: May 22, 2025; Accepted: Jun. 10, 2025; Published: Jun. 13, 2025

Published online at <http://journal.sapub.org/ajcmp>

in nanoparticle obtained can lead to better crystallinity, improving charge carrier mobility in photovoltaic and optoelectronic devices [16]. The present study focuses on one pot synthesis of Zn-CdSeNPs and studies the effects of different doping concentrations of Zn on structural, optical and morphological properties of CdSe nanoparticles used in solar cells. In this study different concentration of Zn was added to CdSe nanoparticles and analyzed using X-ray diffraction (XRD), Ultra violet visible spectroscopy (UV-Vis) and photoluminescence (PL) spectroscopy for structural, optical and electrical properties.

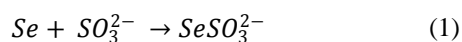
2. Materials and Methods

2.1. Chemicals

All the reagents used were of analytical grade and were purchased from Sigma Aldrich & A.B Chem. Co., Ltd. They include: Cadmium sulphite anhydrous (>95%), anhydrous cadmium chloride (>99%), selenium powder (>99%), L-Cysteine (>99%) and zinc acetate (>99.4%) and deionized water prepared at Murang'a University of Technology Research Laboratory.

2.2. Preparation of Se Ions

0.31g of selenium powder and 1.0g of sodium sulphite in 100 ml of deionized water was refluxed for 8 hours at a temperature of 90°C to form sodium selenosulphate ions as shown in equation 1.



2.3. Synthesis of Zinc Doped Cadmium Selenide Nanoparticles

0.04g of cadmium chloride was dissolved in 50ml of deionized water. L-cysteine was dissolved in cadmium to form a molar ratio of 1:1 L-Cyst/Cd. The pH of the precursor was adjusted to eleven using pH meter. The solution obtained were transferred to three necked flask and stirred continuously. Selenium ions obtained from selenosulphate were added to solution followed by 3, 5, 7, 9, 11 and 15mol% zinc acetate. The solutions obtained were refluxed at a temperature of 90°C for one hour. The nanoparticles obtained were allowed to cool at room temperature for 24 hours then rinsed with ethanol and dried in an oven for one hour at 90°C. The dried nanoparticles were annealed in furnace at a temperature of 250°C.

2.4. Characterization Techniques

The optical properties of Zn-CdSe nanoparticles were determined using Evolution One Plus Model Ultra Violet spectroscopy. Structural and lattice properties of nanoparticles were analyzed using ARL EQUINOX 100 XRD at 40 kV, 0.9mA, at a scanning range of 20-100° degrees at an interval time of 240 seconds. The data obtained were plotted in origin, analyzed and compared to those of standard in Joint committee on powder diffraction standards (JCPDS). Debye

Scherrer equation was used to calculate the crystallite size of the nanoparticles formed. Infitek SP-LF97 photoluminescence spectroscopy was used to determine the luminescence properties and defects in the nanoparticles.

3. Results and Discussion

3.1. X-ray Diffraction (XRD) Analysis

The XRD pattern depicted by pure and Zn doped CdSe nanoparticles is shown in Figure 1(a). The peaks obtained matches those in JCPDS card no 19-0191 associated with zinc blende cubic structure. Doping CdSe with Zn affects its physical, chemical and crystal size properties as demonstrated by color change from dark brown to reddish brown for doped samples. A peak was observed at $2\theta = 33.48$ (marked with *) for 15% Zn doped CdSe nanoparticles. High concentration of dopant causes clustering as shown by peak broadening based on crystal size obtained of (16.99 nm) for 15% at plane (111). 3% Zn-CdSe had the highest intensity and 5% Zn-CdSe nanoparticles had the lowest intensity at peak (111) as shown in Figure 1(b). This means that at 3% Zn doped the nanoparticles were highly crystalline. Doping CdSeNPs increases its crystallinity, similar results has been reported when zinc oxide was doped with magnesium and the XRD pattern showed sharper peaks, indicating better crystal quality [16]. The intensity of the peaks decreased with increased in Zn dopant concentration, this may be attributed by factors such as increased micro strain, introduction of lattice distortion or partial transformation of material to amorphous phase. This observation is uniform with findings reported by Akl et al. (2020) [17] who stated that as disorder increases, the peak intensity decreases reflecting a reduced ability of the crystal lattice to diffract X-rays coherently. Crystal defects occur when Zn is used as dopant in CdSe, this changes the stoichiometry as a result of charge imbalance arising from these defects [18].

Debye Scherrer equation was used to calculate the crystal size of nanoparticles (equation 2) [19]

$$D = \frac{K\lambda}{\beta_{hkl} \cos\theta} \quad (2)$$

D is the crystal size, K is the constant equals to 0.9, the wavelength of the radiation is denoted by λ is 1.54960\AA for copper $K\alpha$ radiation, full width at half maximum (β_{hkl}) and θ is the peak position. The average crystal size of CdSeNPs decreased when doped with Zn, with 15% Zn doped CdSe nanoparticles having a crystal size of 17.72 nm, 3% had 17.60nm and pure CdSeNPs had a crystal size of 24.67nm. This decrease in crystal size with increasing Zn concentration is associated with the fact that Zn limits the agglomeration of CdSeNPs and improves its surface area [20]. It is also possible that Zn^{2+} can substitute Cd^{2+} ions in the lattice of CdSe. Given that the ionic radius of Zn^{2+} (0.74\AA) is smaller than the ionic radius of Cd^{2+} (0.92\AA), this disparity causes a decrease in lattice parameters leading to a smaller crystallite size and more compact crystal structure [21]. The FWHM decreased when doped with 7% Zn, this

indicates an improvement in crystallinity and an increase in crystal size of nanoparticles [22] as observed from the data obtained 7% zinc doped CdSe nanoparticles had an average crystal size of 20.31 nm.

The lattice constant d was calculated using the Bragg's equation

$$n\lambda = 2d_{hkl}\sin\theta \quad (3)$$

For Zinc blende cubic structure $a=b=c$ therefore lattice constant a was calculated using equation 4

$$a = d_{hkl}\sqrt{h^2 + k^2 + l^2} \quad (4)$$

A plot of FWHM against crystal size (D) showed that they were inversely proportional as shown in Figure 2. Smaller crystals have large grain boundaries which broadens the peaks in XRD.

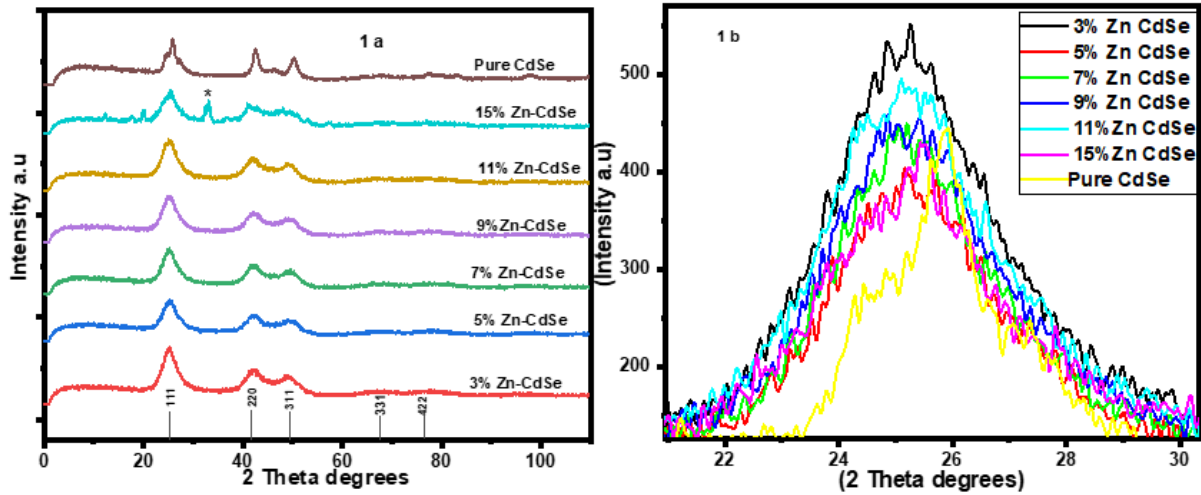


Figure 1. 1(a) XRD spectra of Zn-CdSe and 1(b) enlarged XRD peak [100] of Zn-CdSe nanoparticles

Table 1. Shows the summarized crystal size, lattice constant d , and FWHM of Zn-CdSeNPs with different Zn concentration

Sample	Plane (hkl)	2θ (°)	FWHM (°)	Crystal size (nm)	d_{hkl} (Å)	Lattice parameter a (Å)
Pure CdSe	111	25.3301	4.1701	19.5339	3.5133	6.0854
	220	43.0449	5.1811	16.4810	2.0997	5.9388
	311	49.7662	2.3049	37.9906	1.8307	6.0717
3% Zn-CdSe	111	25.3155	4.4933	18.1190	3.5153	6.0889
	220	42.2967	5.3559	15.9025	2.1351	6.0389
	311	49.0760	4.6436	18.8048	1.8548	6.1516
5% Zn-CdSe	111	25.3566	4.6050	17.6809	3.5097	6.0792
	220	42.3925	4.8942	17.4083	2.1305	6.0259
	311	49.1552	4.5034	19.3964	1.8520	6.1423
7% Zn-CdSe	111	25.3242	4.4466	18.3101	3.5141	6.0868
	220	42.3163	3.6046	23.3163	2.1341	6.0360
	311	49.3325	4.5323	19.2863	1.8458	6.1218
9% Zn-CdSe	111	25.3243	4.6273	17.5946	3.5141	6.0868
	220	42.3661	5.3129	16.0349	2.1317	6.0293
	311	49.0800	4.6065	18.9566	1.8547	6.1513
11% Zn-CdSe	111	25.2688	4.6884	17.3636	3.5217	6.0999
	220	42.3543	6.1273	13.9031	2.1323	6.0310
	311	49.1973	4.2726	20.4476	1.8505	6.1373
15% Zn-CdSe	111	25.1208	4.7884	16.9959	3.5283	6.1114
	220	41.8514	3.4913	24.3591	2.1567	7.9998
	311	48.0237	7.3671	11.8040	1.8930	6.2783

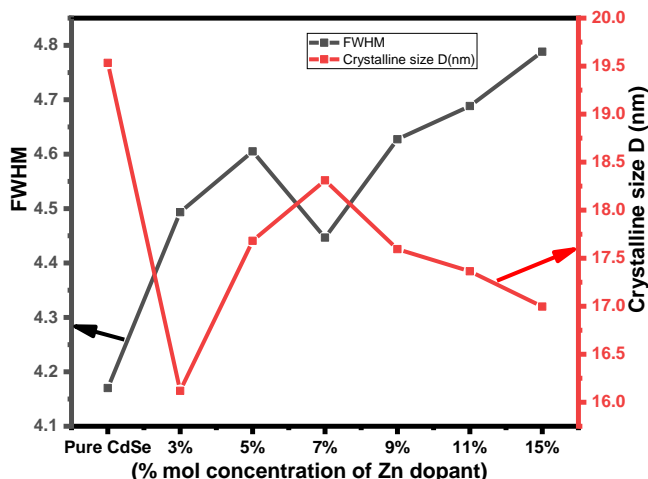


Figure 2. Relationship between FWHM, Crystal size and Zn mol %

3.2. Photoluminescence Spectroscopy

The photoluminescence properties of Zn-CdSe nanoparticles were carried out at an ambient temperature at an excitation wavelength of 400 nm to determine the luminescence properties of Zn-CdSe nanoparticles and their defects. The photoluminescence properties of CdSe were found to be dopant concentration dependant. Figure 3 shows how different concentration of Zn dopant affects the FWHM, peak position and intensity of the peaks in PL. The photoluminescence intensity decreased with increase in dopant concentration and increased at low dopant concentrations. This is associated with the fact that highly doped nanoparticles excite electrons which can return to ground state without emitting photons (non-radiative recombination) [23]. 1% Zn-CdSe nanoparticles had the highest PL intensity and 15% Zn-CdSe nanoparticle had the lowest PL intensity. At high dopant concentration the emission wavelength shift to longer wavelength (red-shift) as a result of lattice strain or dopant induced defects [24]. Blue-shift was observed when low dopant concentration was used, due to quantum confinement effects that occur when

the crystal size decrease the energy gap between conduction band and emission band increase [25]. The dimension of FWHM of PL spectra of samples reflects the distribution of particle size, this can be an efficient method to study size focusing. The FWHM range from 80 to 100nm and decreases with increased in dopant concentration. Narrow FWHM of the PL spectra reflects narrow particle size distribution and this can be used to investigate the size focusing [26].

3.3. Optical Properties

The bandgap energy (E_g) of semi-conductors materials dispersed in liquid with known coefficient is mostly obtained using UV-vis absorption spectroscopy. Figure 4 shows the UV-vis absorbance spectra of Zn-CdSeNPs. The nanoparticles absorbed at different wavelength depending on the amount of dopant used. Highly doped Zn-CdSeNPs (15%) absorbed at higher wavelength (550nm), high concentration of dopant modifies the electronic properties of nanoparticles due to defects that result from stress, strain, interstitial and vacancies defects [27]. Bulk CdSe absorbed at a wavelength of 690nm, the shift towards the shorter wavelength confirms the formation of nanoparticles. Pure CdSe nanoparticle had the lowest absorption band and it absorbed at the lowest wavelength. Similar results were observed by Ca *et al* [28]. Table 2 summarizes the absorption peak and absorption edge for each concentration of dopant.

To obtain the bandgap energy of nanoparticles Tauc's equation 5 [24] was used to estimate the values and a graph plotted.

$$(\alpha h\nu)^\gamma = Ah\nu - AE_g \quad (5)$$

Where E_g is the bandgap energy, A is constant, $h\nu$ is the photon energy, α is absorption coefficient and γ is direct or indirect allowed transition from valence band to conduction band. When γ is 2 it is indirect and when $\frac{1}{2}$ it is direct allowed transition. The plot obtained was extrapolated to intersect the $h\nu$ axis to obtain the bandgap energy. Figure 5 shows the Tauc's plot of different concentration of Zinc dopant.

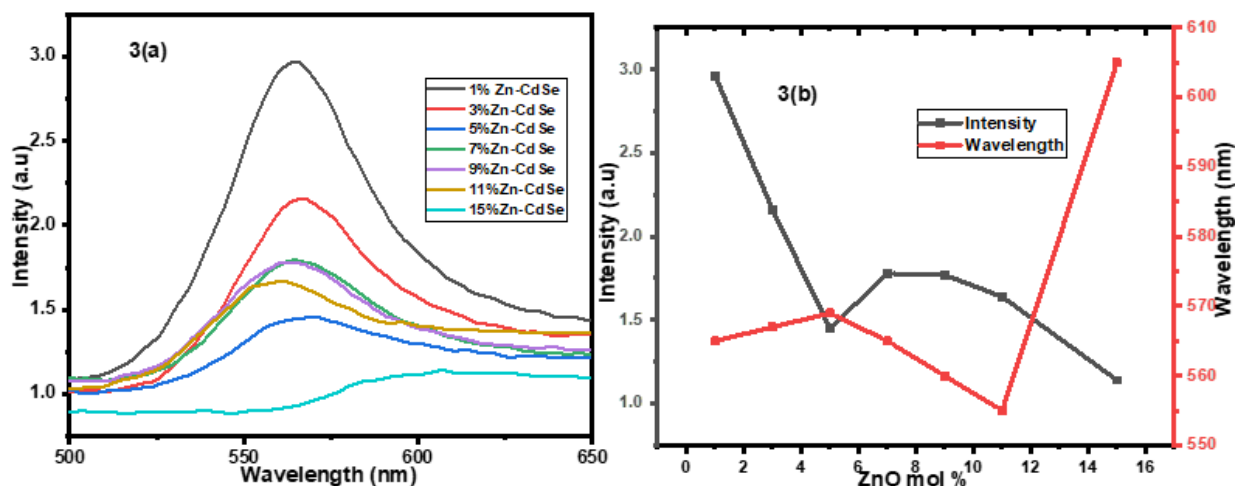


Figure 3. (a) PL emission spectra of varying concentration of Zn-CdSeNPs 3(b) Relationship between PL Intensity, emission wavelength and mol % of Zn dopant in CdSeNPs

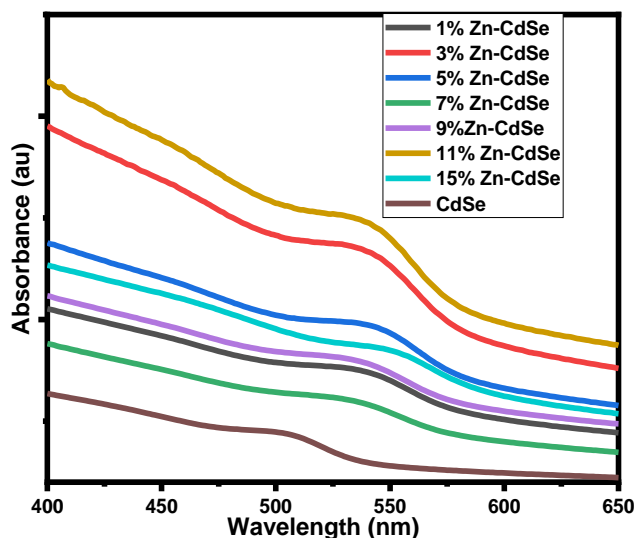


Figure 4. UV-Vis spectra of Zn-CdSe nanoparticles

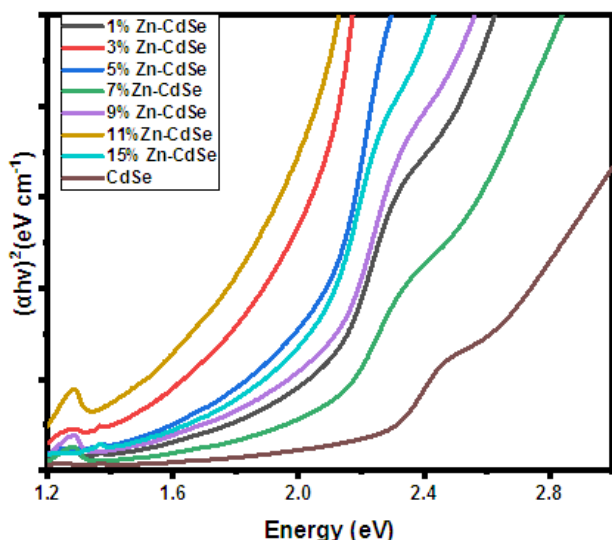


Figure 5. Tauc's plot of Zn-CdSe nanoparticles at varying % Zn mol concentrations

Table 2 shows the bandgap energy obtained when Tauc's plot was extrapolated. The optical properties of CdSe nanoparticles can be tuned by varying the dopant concentration. Increase in bandgap energy at 1% zinc dopant is observed as a result of Zn substituting Cd in CdSe to form $\text{Cd}_x\text{Zn}_{1-x}\text{Se}$ nanoparticle. The bandgap energy of ZnSe is 2.7 eV [29] which is higher compared with 1.74 eV of bulk CdSe, therefore the alloy form has intermediate properties. When high concentration of dopant is added the lattice strain and defects influence the optical properties of nanoparticles thus affecting its bandgap energies. When doped with 15% Zn, tensile strain causes the bandgap energy to decrease. Lattice defects leads to distinct optical features as a results of localized energy state [30]. Other defects from vacancies, dislocation and grain boundaries which are caused by impurities or presence of dopants in the host material are known to cause variation in bandgap energies. Doping CdSe with Zn decreased the bandgap energy from 2.23 to 1.92 eV.

For solar cells applications where the band gap energy required should be lower than the bulk material for ease transition of photons from valence band to conduction band doping CdSe nanoparticle with 11% zinc gives the optimum conditions.

Table 2. Summarized absorption peaks, edge and bandgap energy of Zn-CdSeNPs

$\text{Zn}_x\text{-CdSeNPs}$	Absorption peak (nm)	Absorption edge (nm)	Optical bandgap (eV)
X=0	505	529	2.23
X=1	544	567	1.92
X=3	538	574	1.5
X=5	545	571	1.80
X=7	534	569	2.04
X=9	537	569	1.8
X=11	533	559	1.35
X=15	550	579	1.92

4. Conclusions

Zinc doped Cadmium selenide have been successfully prepared from cadmium chloride and L-cysteine. The XRD results displayed a cubic crystal structure for all the samples. New XRD peaks emerged at higher Zn doping concentrations. The calculated crystallite sizes from the Debye Scherrer generally showed that as the concentration of Zn dopant increase the crystal size decreased from 24.66 to 16.99 nm. The Zinc blende cubic structure of CdSe was retained when dopant was added. The intensity of PL emission was also influenced by doping concentration and the intensity of the peaks decreased with increase in concentration of dopant. The emission wavelength was observed to shift to higher values as the intensity of the peak decreased. 1% zinc doped CdSe nanoparticles had the highest intensity while 15% Zn-CdSe nanoparticles had the lowest PL intensity. The UV-Vis results displayed unique absorption features which varied with changes in the Zn doping concentrations. The bandgap energies obtained from Tauc's plot varied from 2.23 -1.35 eV and 11% Zinc doped CdSe had the smallest bandgap while 1% Zn dopant had the highest bandgap. The structural and optical properties of CdSe nanoparticles are influenced by concentration of dopant which helps in engineering of the material properties of CdSe NPs for a suitable application.

ACKNOWLEDGEMENTS

The author wish to thank Murang'a University of Technology for granting me access to synthesis and characterization equipment.

Conflict of Interest

None.

REFERENCES

- [1] Ashraf, S. A., Siddiqui, A. J., AbdElmoneim, O. E., Khan, M. I., Patel, M., Alreshidi, M., ... & Adnan, M. (2021). Innovations in nanoscience for the sustainable development of food and agriculture with implications on health and environment. *Science of the Total Environment*, 768, 144990.
- [2] Shalaan, E., Ibrahim, E., Al-Marzouki, F., & Al-Dossari, M. J. A. P. A. (2020). Observation of mixed types of energy gaps in some II–VI semiconductors nanostructured films: towards enhanced solar cell performance. *Applied Physics A*, 126(11), 852.
- [3] Kaur, J., & Tripathi, S. K. (2015). Pb dopant induced changes in structural, optical and electrical properties of CdSe thin films. *Journal of Alloys and Compounds*, 622, 953-959.
- [4] Hu, Z., Zhang, X., Xie, C., Wu, C., Zhang, X., Bian, L., ... & Jie, J. (2011). Doping dependent crystal structures and optoelectronic properties of n-type CdSe: Ga nanowires. *Nanoscale*, 3(11), 4798-4803.
- [5] Hassen, M., Riahi, R., Laatar, F., & Ezzaouia, H. (2020). Optical and surface properties of CdSe thin films prepared by sol-gel spin coating method. *Surfaces and Interfaces*, 18, 100408.
- [6] Rose, I., Sathish, R., Rajendran, A. J., & Sagayaraj, P. (2016). Effect of reaction time on the synthesis of cadmium selenide nanoparticles and the efficiency of solar cell. *J. Mater. Environ. Sci*, 7, 1589-1596.
- [7] Wu, B., Lin, Z., Sheng, M., Hou, S., & Xu, J. (2016). Visible-light activated ZnO/CdSe heterostructure-based gas sensors with low operating temperature. *Applied Surface Science*, 360, 652-657.
- [8] Shelke, N. T., Karle, S. C., & Karche, B. R. (2020). Photo-response properties of CdSe thin film photodetector. *Journal of Materials Science: Materials in Electronics*, 31(18), 15061-15069.
- [9] Dupont, E., Koppelaar, R., & Jeanmart, H. (2020). Global available solar energy under physical and energy return on investment constraints. *Applied Energy*, 257, 113968.
- [10] Terricabres-Polo, R., de Bruin, T. A., Kaul, A., van Sark, W. G., & Donega, C. D. M. (2024). Durable Quantum Dot-Based Luminescent Solar Concentrators Enabled by a Photoactive Block Copolymer. *Advanced Energy Materials*, 14(48), 2402375.
- [11] Salem, A., Saion, E., Al-Hada, N. M., Kamari, H. M., Shaari, A. H., Abdullah, C. A. C., & Radiman, S. (2017). Synthesis and characterization of CdSe nanoparticles via thermal treatment technique. *Results in physics*, 7, 1556-1562.
- [12] Bhand, G. R., & Chaure, N. B. (2017). Synthesis of CdTe, CdSe and CdTe/CdSe core/shell QDs from wet chemical colloidal method. *Materials Science in Semiconductor Processing*, 68, 279-287.
- [13] Nahar, L., Esteves, R. J. A., Hafiz, S., Özgür, U., & Arachchige, I. U. (2015). Metal–semiconductor hybrid aerogels: Evolution of optoelectronic properties in a low-dimensional CdSe/Ag nanoparticle assembly. *ACS nano*, 9(10), 9810-9821.
- [14] Mohan, S., Oluwafemi, O. S., Songca, S. P., George, S. C., Miska, P., Rouxel, D., ... & Thomas, S. (2015). Green synthesis of yellow emitting PMMA–CdSe/ZnS quantum dots nanophosphors. *Materials Science in Semiconductor Processing*, 39, 587-595.
- [15] Zhao, F. A., Xiao, H. Y., Bai, X. M., & Zu, X. T. (2019). Effects of Ag doping on the electronic and optical properties of CdSe quantum dots. *Physical Chemistry Chemical Physics*, 21(29), 16108-16119.
- [16] Rani, S., Shanthi, J., Kashif, M., Ayeshamariam, A., & Jayachandran, M. (2016). Studies on different doped Zn concentrations of CdSe thin films. *Journal of Powder Metallurgy & Mining*, 5(1), 1-7.
- [17] Akl, A. A., El Radaf, I. M., & Hassanien, A. S. (2020). Intensive comparative study using X-Ray diffraction for investigating microstructural parameters and crystal defects of the novel nanostructural ZnGa2S4 thin films. *Superlattices and Microstructures*, 143, 106544.
- [18] Pradeev Raj, K., Sadaiyandi, K., Kennedy, A., Sagadevan, S., Chowdhury, Z. Z., Johan, M. R. B & RathinaBala, R. (2018). Influence of Mg doping on ZnO nanoparticles for enhanced photocatalytic evaluation and antibacterial analysis. *Nanoscale research letters*, 13, 1-13.
- [19] Rani, S., Shanthi, J., Kashif, M., Ayeshamariam, A., & Jayachandran, M. (2016). Studies on different doped Zn concentrations of CdSe thin films. *Journal of Powder Metallurgy & Mining*, 5(1), 1-7.
- [20] Waweru, G. S., Kiprotich, S., & Waithaka, P. (2024). Effects of different Zn doping concentration on the optical and structural properties of TiO2 nanoparticles.
- [21] Asere, T. G., & Du Laing, G. (2020). Zn-doped CdSe nanoparticles: Impact of synthesis conditions on photocatalytic activity. *Environmental Technology & Innovation*, 20, 101126.
- [22] Kiprotich, S., Dejene, F. B., Ungula, J., & Onani, M. O. (2016). The influence of reaction times on structural, optical and luminescence properties of cadmium telluride nanoparticles prepared by wet-chemical process. *Physica B: Condensed Matter*, 480, 125-130.
- [23] Thirugnanam, N., & Govindarajan, D. (2016). Aqueous synthesis and characterization of Ni, Zn co-doped CdSe QDs. *International Nano Letters*, 6, 105-109.
- [24] Asere, T. G., & Du Laing, G. (2020). Zn-doped CdSe nanoparticles: Impact of synthesis conditions on photocatalytic activity. *Environmental Technology & Innovation*, 20, 101126.
- [25] Hamizi, N. A., Johan, M. R., Chowdhury, Z. Z., Wahab, Y. A., Al-Douri, Y., Saat, A. M., & Pivezhzani, O. A. (2018). Optical structure modification induced by lattice strain in Mn-doped CdSe QDs. *Optical Materials*, 86, 441-448.
- [26] Zaini, M. S., Ying ChyiLiew, J., Alang Ahmad, S. A., Mohmad, A. R., & Kamarudin, M. A. (2020). Quantum confinement effect and photo enhancement of photoluminescence of PbS and PbS/MnS quantum dots. *Applied Sciences*, 10(18), 6282.
- [27] Zhu, Z., Shao, H., Dong, X., Li, N., Ning, B. Y., Ning, X. J., ... & Zhuang, J. (2015). Electronic band structure and sub-band-gap absorption of nitrogen hyperdoped silicon. *Scientific reports*, 5(1), 10513.

- [28] Ca, N. X., Van, H. T., Do, P. V., Thanh, L. D., Tan, P. M., Truong, N. X., ... & Hien, N. T. (2020). Influence of precursor ratio and dopant concentration on the structure and optical properties of Cu-doped ZnCdSe-alloyed quantum dots. *RSC advances*, 10(43), 25618-25628.
- [29] Imran, M., Saleem, A., Khan, N. A., Khurram, A. A., & Mehmood, N. (2018). Amorphous to crystalline phase transformation and band gap refinement in ZnSe thin films. *Thin Solid Films*, 648, 31-38.
- [30] Böer, K. W., & Pohl, U. W. (2023). Optical properties of defects. In *Semiconductor Physics* (pp. 703-753). Cham: Springer International Publishing.